IL NUOVO CIMENTO Vol. 35 C, N. 2 Marzo-Aprile 2012
DOI 10.1393/ncc/i2012-11209-6

Colloquia: Transversity 2011

HERMES results on hard exclusive processes

S. Yaschenko on behalf of the HERMES Collaboration
DESY, Zeuthen - Platanenallee 6, D-15738, Germany

ricevuto il 9 Novembre 2011; approvato l'11 Gennaio 2012
pubblicato online il 26 Marzo 2012

Summary. — Hard exclusive leptoproduction of real photons or mesons on nucleons and nuclei can provide access to Generalized Parton Distributions (GPDs). The theoretical framework of GPDs includes parton distribution functions and form factors as limiting cases and as moments of GPDs, respectively, and can provide a multidimensional representation of the structure of hadrons at the partonic level. The HERMES experiment at DESY, Hamburg, collected a wealth of data on Deeply Virtual Compton Scattering (DVCS) and exclusive meson production utilizing the HERA polarized electron or positron beams with an energy of 27.6 GeV and longitudinally and transversely polarized or unpolarized gas targets (H, D or heavier nuclei). The azimuthal asymmetries measured in the DVCS process allow access to the imaginary and/or real part of certain combinations of GPDs. For the last two years of HERA running, the HERMES collaboration installed a recoil detector to improve the selection of DVCS events by direct measurement of the recoil protons. An overview of recent HERMES results on DVCS including first results obtained with the recoil detector is presented.

PACS 13.60.-r – Photon and charged-lepton interactions with hadrons.
PACS 13.88.+e – Polarization in interactions and scattering.

1. – Introduction

The soft, non-perturbative part of hard exclusive reactions is described in terms of Generalized Parton Distributions (GPDs) [1-3]. These distributions include parton distribution functions and form factors as limiting cases and moments of GPDs, respectively. GPDs provide a multidimensional picture of the nucleon, correlating the longitudinal momentum fraction of partons with their transverse distance from the nucleon's center. Furthermore, moments of certain GPDs were found to be directly related to the total (including orbital) angular momentum carried by partons in the nucleon [4]. GPDs are accessible through exclusive processes that involve at least two hard vertices, yet leave the target nucleon intact. GPDs depend on three kinematic variables: the squared four-momentum transfer t to the nucleon and x and ξ, which represent respectively the average and half the difference of the longitudinal momentum fractions carried by the

probed parton in initial and final states. For the proton, a spin-$\frac{1}{2}$ target, there are four twist-2 GPDs per quark flavor: H, E, $\widetilde{H}$ and $\widetilde{E}$, while for the deuteron, a spin-1 target, nine GPDs are required: $H_1, H_2, H_3, H_4, H_5, \widetilde{H}_1, \widetilde{H}_2, \widetilde{H}_3, \widetilde{H}_4$. Among other hard exclusive processes, Deeply Virtual Compton Scattering (DVCS) is one of the theoretically cleanest ways to access GPDs. DVCS process is experimentally indistinguishable from the electromagnetic Bethe-Heitler (BH) process because they have identical initial and final states. The real photon is radiated from the struck quark in DVCS, or from the initial or scattered lepton in BH.

The cross-section of the exclusive leptoproduction of a real photon reads as [5]

$$\frac{\mathrm{d}\sigma}{\mathrm{d}x_B \mathrm{d}Q^2 \mathrm{d}t \mathrm{d}\phi} = \frac{\alpha^3 x_B y}{16\pi^2 Q^2 e^3} \frac{2\pi y}{Q^2} \frac{|T_{DVCS}|^2 + |T_{BH}|^2 + I}{\sqrt{1 + 4x_B^2 M_N^2/Q^2}}, \tag{1}$$

where T_{DVCS} (T_{BH}) is the DVCS (BH) amplitude, I is the interference term, x_B is the Bjorken scaling variable and $-Q^2$ is the squared four-momentum transferred by the virtual photon. The amplitude of the BH process can be precisely calculated from measured elastic form factors of the nucleon. The BH process dominates at HERMES kinematics. However, the kinematic dependences of the cross-section terms generate a set of azimuthal asymmetries which depend on the azimuthal angle ϕ between the real-photon production plane and the lepton scattering plane. In the case of a transversely polarized target, asymmetries can, in addition to ϕ, also depend on the angle ϕ_S between the lepton scattering plane and the direction of the target polarization vector.

Using data collected with longitudinally polarized electron/positron beam with different target polarization states, it is possible to measure asymmetries with respect to beam charge, beam polarization and target polarization alone and also with respect to their different combinations.

As an example, the cross-section for a longitudinally polarized lepton beam scattered off an unpolarized proton target σ_{LU} can be related to the unpolarized cross-section σ_{UU} by

$$\sigma_{LU}(\phi; P_B, C_B) = \sigma_{UU}(\phi) \cdot \left[1 + P_B A_{LU}^{DVCS}(\phi) + C_B P_B A_{LU}^{I}(\phi) + C_B A_C(\phi)\right], \tag{2}$$

where A_{LU}^{I} (A_{LU}^{DVCS}) is the charge (in)dependent beam-helicity asymmetry (BSA) and A_C is the beam charge asymmetry (BCA), $C_B(P_B)$ denotes the beam charge (polarization). In the analysis, effective asymmetry amplitudes are extracted, which include ϕ dependencies from the BH propagators and the unpolarized cross-section. Each asymmetry can be expanded in a Fourier series in ϕ as

$$A_{LU}^{I}(\phi) = \sum_{n=1}^{2} A_{\mathrm{LU,I}}^{\sin(n\phi)} \sin(n\phi) + \sum_{n=0}^{1} A_{\mathrm{LU,I}}^{\cos(n\phi)} \cos(n\phi), \tag{3}$$

$$A_{LU}^{DVCS}(\phi) = \sum_{n=1}^{2} A_{\mathrm{LU,DVCS}}^{\sin(n\phi)} \sin(n\phi) + \sum_{n=0}^{1} A_{\mathrm{LU,DVCS}}^{\cos(n\phi)} \cos(n\phi), \tag{4}$$

$$A_C(\phi) = \sum_{n=0}^{3} A_{\mathrm{C}}^{\cos(n\phi)} \cos(n\phi) + A_{\mathrm{C}}^{\sin\phi} \sin\phi. \tag{5}$$

The amplitudes were fitted simultaneously using a Maximum Likelihood method described in detail in ref. [6]. Asymmetries amplitudes are expressed in terms of different

combinations of Compton Form Factors (CFFs) [5], which are convolutions of hard scattering coefficient functions with corresponding GPDs.

2. – Experiment and data analysis

The HERMES experiment [7] utilized longitudinally polarized 27.6 GeV electron or positron beams of the HERA storage ring at DESY together with longitudinally and transversely polarized or unpolarized gas targets (H, D or heavier nuclei). In the winter shutdown 2005/2006 the HERMES spectrometer was upgraded in the target region with a Recoil detector to improve the selection of events from exclusive processes. The Recoil detector comprised a set of silicon strip detectors (SSD) located inside the HERA beam vacuum, surrounded by a scintillating-fiber tracker (SFT), a photon detector (PD), and a 1 Tesla superconducting magnet. Commissioning of the Recoil detector started in spring 2006 when part of the detector was already operational and finished in fall 2006 resulting in stable running of the detector until the HERA shutdown in July of 2007. For the results obtained with the Recoil detector, positron beam data from 2006 and 2007 collected with an unpolarized hydrogen target and the fully operational Recoil detector were used. The bent tracks of charged particles with momenta from 0.125 GeV/c to 1.4 GeV/c are reconstructed in the Recoil detector using coordinate information from the SSD and the SFT. For protons, momentum reconstruction is significantly improved by taking energy deposits in the SSD into account.

Event candidates are selected requiring the detection of exactly one scattered positron and exactly one photon. In addition, information about all tracks reconstructed in the Recoil detector is used, if available.

For data without Recoil detector information, the selection of DVCS/BH events was performed by requiring the missing mass, calculated using the lepton and the photon 3-momenta, to be equal to the proton mass within the resolution of the spectrometer, which defined the "exclusive region" of the data sample. For such "unresolved" event sample, it is not possible to separate the pure DVCS/BH events from the "associated" process, where the nucleon in the final state is excited to a resonant state. Within the exclusive region, its contribution is estimated from a Monte Carlo simulation to be about 12% of the signal. The main background contribution of about 3% originates from semi-inclusive π^0 production and is corrected for. The contribution from exclusive π^0 production is estimated to be less than 0.5%.

For data with Recoil detector information, kinematic event fitting was performed for every DVCS event candidate by using the measured 3-momenta of the electron, the photon and the proton candidate detected in the Recoil detector under the hypothesis that the process is pure DVCS/BH, *i.e.* $ep \to ep\gamma$. Applying a cut on the probability that a particular event satisfies this hypothesis, one can select pure DVCS/BH events with high efficiency and low background contamination. It was demonstrated from detailed Monte Carlo studies that the contamination of the background from the associated process is below 0.1%. The background from semi-inclusive and exclusive π^0 production is estimated to also be negligible. It should be noted that the kinematic acceptance for this "pure" event sample is different from the acceptance for the unresolved event sample, especially for small values of $-t$.

In order to compare results under similar kinematic conditions, a "reference" event sample was created. For the reference sample, in addition to the selection criteria used for the unresolved sample, a "hypothetical" proton with 3-momenta calculated from the 3-momenta of electron and photon was required to be in the Recoil detector acceptance.

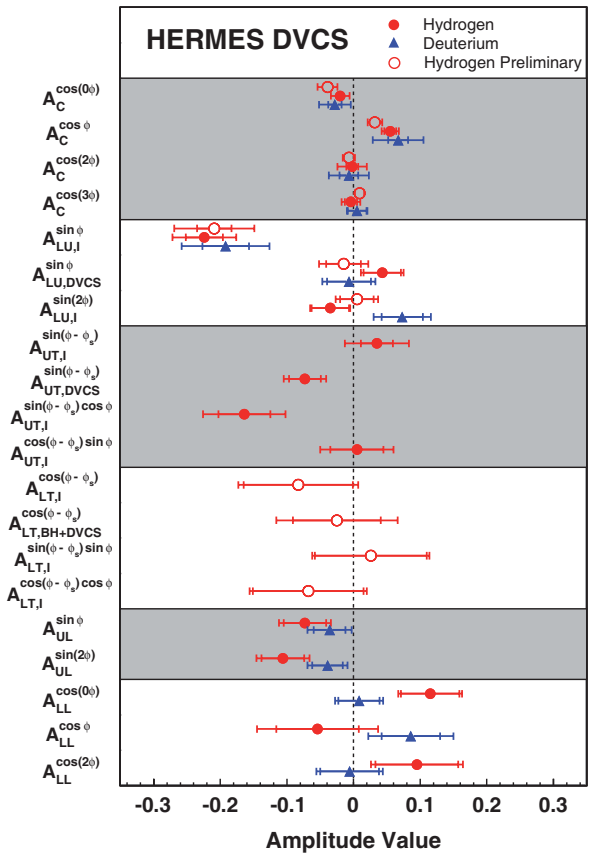

Fig. 1. – Overview of all DVCS azimuthal asymmetry amplitudes measured at HERMES.

For this subsample, background conditions are very similar to those for the unresolved sample. So that it can be used to understand and to compare to the background-free measurement.

The systematic uncertainties are obtained from a Monte Carlo simulation estimating the effects of limited acceptance, smearing and finite bin width. There are additional scale uncertainties arising from the uncertainty in the measurement of the beam or target polarizations.

3. – Results

Figure 1 presents an overview of all azimuthal asymmetry amplitudes integrated over the entire HERMES kinematic range using the data taken in the years 1996–2007. This includes data on the unpolarized hydrogen [8] and deuterium [9] targets, the longitudinally polarized hydrogen [10] and deuterium [11] targets and the transversely polarized hydrogen [6,12] target. The beam-charge asymmetry amplitude $A_C^{\cos\phi}$ and the beam-spin asymmetry amplitude $A_{LU,I}^{\sin\phi}$, sensitive to the interference term, show a significant non-zero value. These two amplitudes are sensitive to the real and imaginary parts of CFF $\mathcal{H}$, respectively. For the case of deuterium target the leading amplitudes of beam-charge and

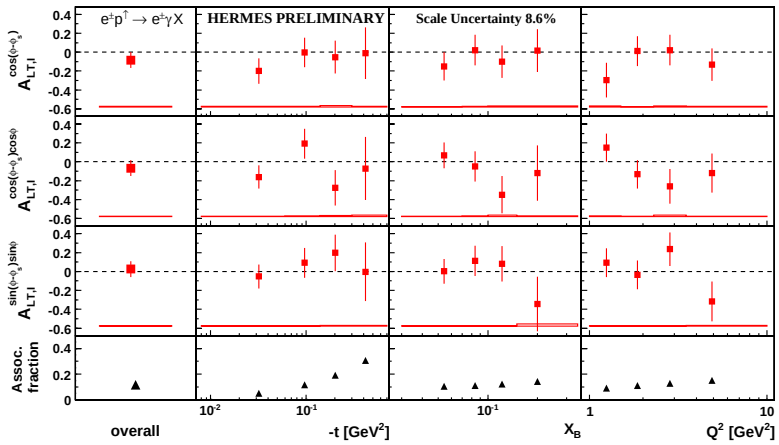

Fig. 2. – The leading amplitudes of transverse double-spin asymmetries $A_{LT,I}(\phi, \phi_S)$.

beam-helicity asymmetries are sensitive respectively to the real and imaginary parts of CFF $\mathcal{H}_1$. The results on both targets are compatible within the total experimental uncertainties. The amplitude $A_{LU,DVCS}^{\sin\phi}$, sensitive to the squared DVCS amplitude, is found to be compatible with zero. In the bottom panels of fig. 1, the results on the longitudinal

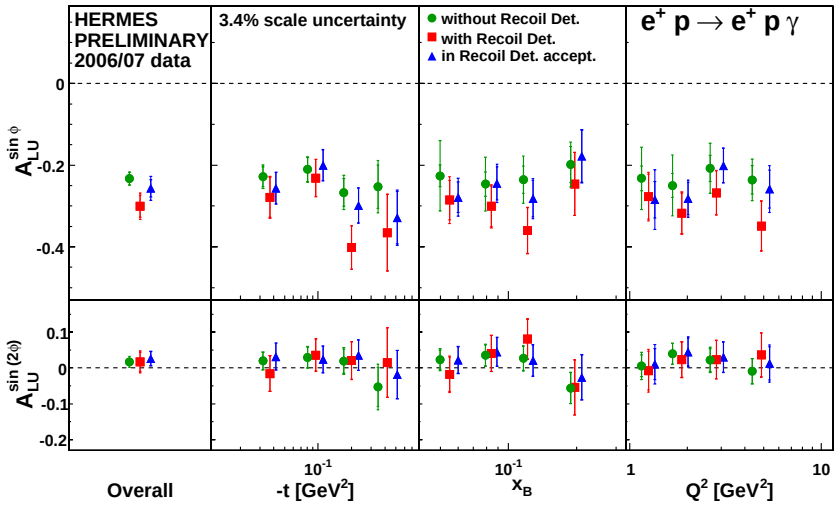

Fig. 3. – (Colour on-line) The $\sin(n\phi)$ asymmetry amplitudes of the DVCS single-charge beam-helicity asymmetry of the pure (red squares), reference (blue triangles) and unresolved (green circles) samples extracted from 2006 and 2007 hydrogen data taken with a positron beam and fully operational Recoil detector in projections *versus* $-t$, x_B, and Q^2 and also integrated over the entire acceptance (overall). The inner error bars denote the statistical uncertainties and the total error bars the quadratic sum of the statistical and systematic uncertainties.

single-target-spin $A_{UL}(\phi)$ and double-spin $A_{LL}(\phi)$ asymmetries [10, 11] are presented. For the case of hydrogen target, the leading amplitudes of these asymmetries are sensitive to the imaginary and real parts of CFF $\widetilde{\mathcal{H}}$, respectively, while for the deuterium target they are sensitive to CFF $\widetilde{\mathcal{H}}_1$. The results obtained on both targets are compatible within the total experimental uncertainties. Also shown in fig. 1 are the leading amplitudes of transverse-target-spin asymmetry, measured on hydrogen target [6]. The amplitude $A_{UT,I}^{\sin(\phi-\phi_S)\cos(\phi)}$ that has significant negative value, is sensitive to the imaginary part of CFF $\mathcal{E}$, while the real part of CFF $\mathcal{E}$ can be accessed through measurement of transverse-double-spin asymmetries. Preliminary results [12] on the leading amplitudes of double-spin asymmetries are shown in fig. 1 in entire HERMES kinematics and in fig. 2 in projections *versus* $-t$, x_B and Q^2. The error bars (bands) represent the statistical (systematic) uncertainties. The results of double-spin asymmetries are consistent with zero over almost all kinematic regions. In the bottom panel of fig. 2 relative contribution of associated processes that were obtained by Monte Carlo simulations is shown.

In fig. 3, preliminary results [13] on the $\sin(n\phi)$-amplitudes of the DVCS single-charge beam-helicity asymmetry extracted from 2006 and 2007 hydrogen data taken with a positron beam and fully operational Recoil detector are shown in projections *versus* $-t$, x_B, and Q^2 and also integrated over the entire acceptance. Results are presented for the pure sample, the reference sample, and the unresolved sample.

While the leading $\sin\phi$ amplitude shows no dependence on x_B and Q^2 in either sample, there is an indication for a non-flat behavior *versus* $-t$ for the pure sample. For low values of $-t$, the pure and the reference sample containing a mixture of processes deliver results that are compatible within uncertainties. For higher values of $-t$, the pure amplitude shows a trend of a larger magnitude than that of the reference amplitude. The overall value of the sub-leading $\sin(2\phi)$-amplitude is compatible with zero within its statistical uncertainty for all samples. It is difficult to draw a solid conclusion about any distinctive kinematic dependence. There is no large difference of the results for the pure sample with the results for the reference and unresolved samples as well as with previously published results [8]. There is an indication that the pure DVCS/BH amplitude is larger in magnitude. This difference may be attributed to the removal of associated processes from the pure sample.

REFERENCES

[1] Müller D. *et al.*, *Fortschr. Phys.*, **42** (1994) 101.
[2] Radyushkin A. V., *Phys. Lett. B*, **380** (1996) 417.
[3] Ji X., *Phys. Rev. D*, **55** (1997) 7114.
[4] Ji X., *Phys. Rev. Lett.*, **78** (1997) 610.
[5] Belitsky A. V., Müller D. and Kirchner A., *Nucl. Phys. B*, **629** (2002) 323.
[6] Airapetian A. *et al.* (HERMES Collaboration), *JHEP*, **06** (2008) 066.
[7] Ackerstaff K. *et al.* (HERMES Collaboration), *Nucl. Instrum. Methods A*, **417** (1998) 230.
[8] Airapetian A. *et al.* (HERMES Collaboration), *JHEP*, **11** (2009) 083.
[9] Airapetian A. *et al.* (HERMES Collaboration), *Nucl. Phys. B*, **829** (2010) 1.
[10] Airapetian A. *et al.* (HERMES Collaboration), *JHEP*, **06** (2010) 019.
[11] Airapetian A. *et al.* (HERMES Collaboration), *Nucl. Phys. B*, **842** (2011) 265.
[12] Airapetian A. *et al.* (HERMES Collaboration), arXiv:1106.2990 (hep-ex) (2011).
[13] Bowles J., Riedl C. and Yaschenko S. for the HERMES Collaboration, *Proceedings of 19th International Workshop On Deep-Inelastic Scattering And Related Subjects (DIS 2011), Newport News, Virginia, USA, 2011.*